Physiology and Molecular Biology of Plants (September 2024) 30(9):1429–1447
https://doi.org/10.1007/s12298-024-01508-8

RESEARCH ARTICLE

Green synthesis and characterization of Fe_2O_3, ZnO and TiO_2 nanoparticles and searching for their potential use as biofertilizer on sunflower

Tuğba Özgören Can[1] · Yıldız Aydin[2] · Güldem Utkan[3] · Ahu Altınkut Uncuoğlu[1]

Received: 10 May 2024 / Revised: 9 July 2024 / Accepted: 2 September 2024 / Published online: 12 September 2024

Abstract

Nanoparticles, thanks to their superior properties such as large surface area and high reactivity, can be an alternative to traditional fertilizers for improving nutrient uptake. Furthermore, considering that chemical and physical synthesis methods require high energy consumption and cause environmental pollution, plant-mediated green synthesis of NPs has attracted great attention since it provides eco-friendly, biocompatible, and inexpensive solutions. In this present study, plant mediated green synthesis of Iron Oxide (Fe_2O_3), Zinc Oxide (ZnO) and Titanium Dioxide (TiO_2) nanoparticles by using *Laurus nobilis* leaves (bay leaves) were carried out and their structural properties were characterized by UV visible spectra, Dynamic Light Scattering (DLS), Fourier Transform Infrared (FTIR), X-Ray Diffraction (XRD) and Transmission Electron Microscopy (TEM). UV spectrum and FTIR analysis exhibited characteristic peaks indicating the presence of the desired NPs, while DLS analysis and TEM images confirmed that synthesized particles are in nano-scale. The potential of nanoparticles as biofertilizer in agricultural uses were assessed by investigating their effects on sunflower growth in hydroponic system. TEM images of the NP applied plant tissues proved the uptake and translocation of NPs from root to leaf. Furthermore, Fe_2O_3, ZnO and TiO_2 NP applications on sunflower up to 5 ppm generally improved physiological growth parameters such as root length, fresh weight and leaf surface area while 20 ppm of Fe_2O_3 and ZnO NPs application cause a significant decrease.

✉ Ahu Altınkut Uncuoğlu
ahu.uncuoglu@marmara.edu.tr

[1] Department of Bioengineering, Faculty of Engineering, Marmara University, Istanbul, Türkiye

[2] Department of Biology, Faculty of Science, Marmara University, Istanbul, Türkiye

[3] SUNUM Nanotechnology Research Center, Sabanci University, Istanbul, Türkiye

Graphical abstract

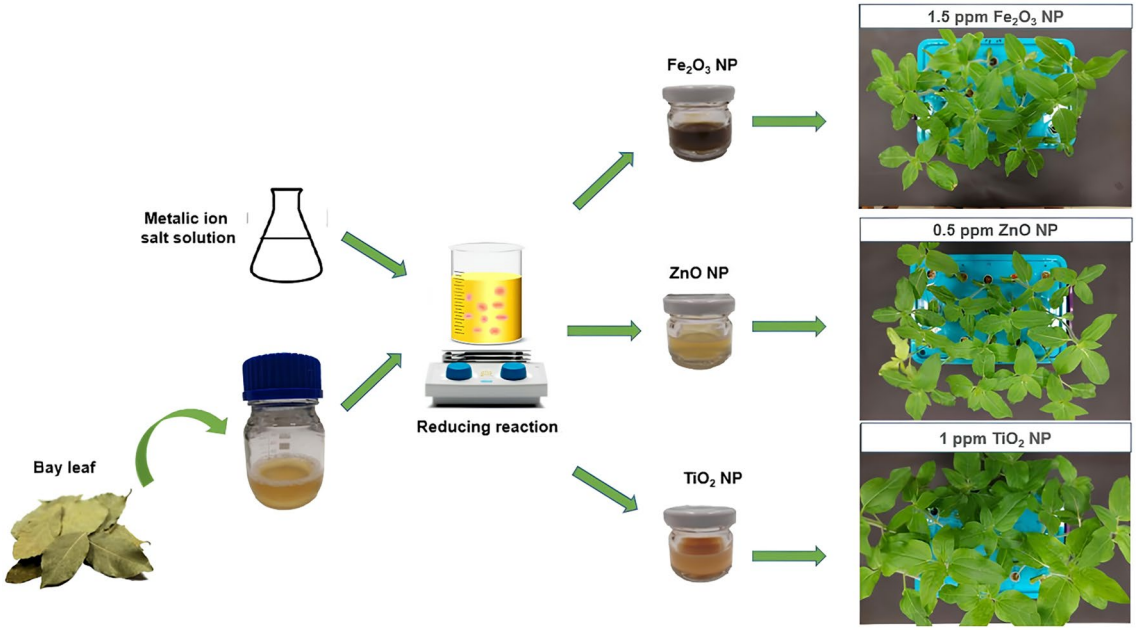

Keywords Metallic nanoparticle · Plant mediated green synthesis · Nanofertilizer · Sunflower

Introduction

Global demand for food and agricultural products are rising due to the rapidly increasing world population (Ashraf et al. 2021) while several factors such as intense agriculture, soil fertility loss, environmental stresses (heat, drought, salinity, cold, metals) and nutrient imbalance in the shadow of global warming significantly decreased sustainable agriculture and plant production (Tauqeer et al. 2022). In additon, a worldwide outbreak Covid19 pandemic has brought about a rising awareness among people for safe food and agricultural products (Alamdari et al. 2022). In order to meet the needs of the rapidly growing population of the world in terms of high quality food supply and increased crop production with sustainable agricultural solutions, the use of modern technologies as alternative to current practices is of great importance.

Nanotechnology at this point, has been emerged as a cornerstone technology for the transformation of conventional food and agricultural industries for sustainable farming, better food quality and safety (Ashraf et al. 2021). Food additives with high nutritional value, intelligent antibacterial food packages, nanosensores for the detection of food-borne pathogens are some of examples to its applications in food industry (Ashraf et. al 2021; Alamdari et al. 2022). Furthermore, nanomaterials are used to increase the productivity and sustainability in agricultural applications with less input and less waste compare to current approaches (Gangwar et al. 2023). As alternative to traditional fertilizers, which cause environmental pollution when applied to agricultural lands in large quantities for long time, nanoparticles (NPs) have superior properties such as high reactivity, good conductivity and strength thanks to their small size and large surface area (Kolenčík et. al. 2020; Gutiérrez-Ramírez et. al. 2021). It is thought that NPs could improve nutrient uptake and contribute to plant durability against several stress conditions (Abobatta 2018; Gangwar et al. 2023). Numerous studies in the literature have highlighted the beneficial impacts of SiO_2, CeO_2, TiO_2, Fe, and ZnO nanoparticles on various aspects such as plant growth, seed germination, and the antioxidative defense system across several plant species, including sunflower (Janmohammadi et al. 2017; Tassi et al. 2017; Verma et al. 2018; Lahuf et. al 2019; Kolenčík et. al. 2020).

Sunflower (*Helianthus annuus* L.) is one of the most prominent oilseed crops around the world (Badouin et al. 2017; Hussain et al. 2018). It ranks fourth after palm oil, soybean, and canola oil, comprising up to 12% of global production (Dimitrijevic and Horn 2018). Due to the high content of mono- and polyunsaturated fatty acids and vitamin E in its seeds, sunflower provides high-quality oil, making it desirable (Kaya et al. 2012). Its seeds are not only rich in oil but also protein (around 16%), thus competing in markets for both vegetable oils and protein-rich products such as soybean (Pilorgé 2020). Furthermore, sunflower is also used

as a source of antimicrobial, anti-inflammatory, antitumor, and antioxidant agents in medicinal applications, thanks to its phytochemical content such as vitamins, tocopherols, flavonoids, carotenoids, alkaloids, and phenolic acids. It is also known that sunflower has positive effects on blood pressure control, skin protection, and lowering cholesterol (Adeleke and Babalola 2020).

Especially in the shadow of global warming and rapid population growth, the demand for sunflower will continue to increase due to its high tolerance to different environmental conditions, including drought (Badouin et al. 2017). However, the rapid increase in the world population and climate change threaten the stable supply of food production, including sunflower oil, on a global scale. Poor soil fertility (lack of essential minerals), disease attacks, and pesticide infestations are some of the major constraints that affect sunflower production yield (Gulya et al. 2019; Adeleke and Babalola 2020). Several control strategies have hitherto been developed, including chemical fertilizer utilization, soil solarization, herbicide and biological agent utilization, modification of planting times, crop rotation, and genetic breeding (Pérez-Vich et al. 2004; Louarn et al. 2016). In addition to these current methods, the use of modern technologies is of great importance in order to increase crop yield. Many studies in literature revealed that several nanoparticle applications with appropriate doses improved the growth and yield parameters in sunflower.

Although iron is a major microelement with vital importance in several actions within the plant cell, such as respiration, photosynthesis, DNA synthesis, and hormone production, its deficiency in plants is a common problem that causes chlorosis (Blamey et al. 1997). Kabir et al. (2021) have revealed a significant decrease in parameters related to photosynthesis and shoot and root morphology of sunflower in the presence of iron depletion. In this respect, studies have shown that the application of iron in different forms, such as Fe_3O_4 and Fe_2O_3 nanoparticles, positively affects several growth parameters (Alidoust and Isoda 2013; Li et al. 2016). ZnO, another essential micronutrient utilized by plants, is crucial for many enzymes and stabilizes the structure of proteins and membranes (Said and Mohamed Noaman 2021). It also plays important roles in auxin and indole acetic acid synthesis from tryptophan, chlorophyll synthesis, and biochemical reactions required for carbohydrate formation. It organizes the stomatal functions of the cells by maintaining the potassium content constant. Hence, the lack of Zn considerably affects crop quality and yield. A study carried out by Rajiv et al. (2013) revealed that foliar application of ZnO nanoparticles to sunflower positively affects growth and seed yield. Another study has shown that ZnO has an inhibiting effect on *Rhizoctonia solani*, a pathogenic fungus that causes damping-off disease in sunflower (Lahuf et al. 2019). Although Ti is not an essential nutrient for plants, there are studies indicating that TiO_2 photocatalytic nanoparticles affect metabolic activities, light energy conversion, and the activity of enzymatic antioxidant factors. Janmohammedi et al. (2017) revealed that TiO_2 NP application to sunflower enhances growth parameters such as plant height, leaf length, stem diameter, etc. Additionally, studies by Sabaghnia et al. (2018) showed that TiO_2 foliar application increases crop yield in sunflower.

While chemical or physical fabrication methods could be utilized for NPs production, they can be also synthesized with the aid of biological entities such as plants, microbes, fungi, algea. Biological molecules synthesized by these living organisms can serve as reducing agents to fabricate NPs. Considering chemical and physical methods requires high energy consumption and cause environmental pollution, biological (green) synthesis of NPs have attracted a great attention since it provides eco-friendly, biocompatible and cheap solutions. Among these entities, synthesis via plant extracts with high natural surfactant content (Alamdari et al. 2020) is commonly prefered due to its advantages in terms of inexpensive cost and rapid reaction time. The working process of NP synthesis via plants is quite simple. After biologically active compounds of plants are extracted into water, a metallic ion salt solution is mixed with this extract at ambient temperatures and reduction to metallic NPs occur (Mystrioti et al. 2016; Ishak et al. 2019). Alamdari et al. (2020) reported that characterization studies showed that ZnO NPs using leaf extract of *Sumbucus ebulus* with better antibacterial activity was succesfully synthesized. Bay leaf (*Laurus nobilis*) is another type of plant that can be used for the green synthesis of nanoparticles. It has been used as spice all around the world and it is also getting more attention as a medicinal and aromatic plant due to its several properties. In addition to its rich essential oil content in its leaves, it also contains sesquiterpene lactones, several flavonoids like kaempferol and alkaloids such as eucalyptol, limonene, α-tocopherol, β –sitosterol, eugenol (Chemingui et al. 2019). These contents make bay leaf desirable for the green synthesis of NPs to be used as reducing agent.

In the light of all this information, in this study, plant mediated green synthesis of Iron Oxide (Fe_2O_3), Zinc Oxide (ZnO) and Titanium Dioxide (TiO_2) nanoparticles by using *Laurus nobilis* leaves was performed and their potential as biofertilizers were investigated by examining their effect on growth parameters of sunflower. This is the first study investigating the uptake of *Laurus nobilis* mediated green synthesized metallic nanoparticles and their effect on some growth parameters after NP application to sunflower in hydroponic system. Unlike other studies, NPs in their reaction mixture without any purification step were directly added in the hydroponic system. Thus, the aim was to improve the stability of NPs in the presence of bay leaf extract as a capping agent. As a result

of the study, TEM images from NP applied plant sections confirmed the translocation of NP from roots to the leaves and positive effects of all NPs up to a certain dose application were obtained while their increasing doses cause toxicity.

Materials and method

Materials

For the green synthesis of NPs, $FeCl_3 \cdot 6H_2O$ and $C_4H_6O_4Zn \cdot 2H_2O$ were purchased from Isolab Chemicals and $C_{12}H_{28}O_4Ti$ from Acros Organics as NP precursors. Bay leaves (*Laurus nobilis* L.) were supplied from a local market as NP reducing agent. *Orobanche cumana* and *Plasmopara halstedii* sensitive linoleic sunflower line IMI 044 B as plant material used in NP applications were supplied from Trakya Agricultural Research Institute. Hoagland medium as nutrient source was used for hydroponic system (Hoagland and Arnon 1950).

Green synthesis of nanoparticles

To be used as reducing agent in green synthesis, dried leaves of *Laurus nobilis* were extracted according to the protocol given by Moosa and Jafaar (2017) with some modifications. Bay leaves were washed and dried at room temperature. After 5 g of bay leaves were blended and mixed with 100 ml ultra pure water, the mixture was boiled on hotplate for 5 min. After it was cooled to room temperature, plant residues were filtered through No. 1 Whatman filter paper and centrifuged at 4000 × g for 10 min.

0.1 M $FeCl_3 \cdot 6H_2O$, 0.2 M $C_4H_6O_4Zn \cdot 2H_2O$ and 0.1 M $C_{12}H_{28}O_4Ti$ solutions were prepared as precursors for Fe_2O_3, ZnO and TiO_2 NPs, respectively. Then, plant extract and precursor were mixed for NP formation with 4:6 ratio and the mixtures were sonicated for 1 h at 50 °C. Finaly, the mixtures for Fe_2O_3 and ZnO NP were shaked at 150 rpm for 1.5 h at room temperature while overnight shaking was performed for TiO_2 NPs with the same conditions (Beheshtkhoo 2018; Hussain 2019; Sethy 2020).

Characterization of synthesized nanoparticles

Bay leaf mediated NPs were scanned with UV/Vis spectrophotometer (Beckman Coulter, DU 730) between 200 and 800 nm wavelengths for determination of maximum absorption peaks. Size and size distribution of nanoparticles were determined via Malvern ZX Zetasizer. Dilution with distilled water was performed when the measurements are out of range. The morphology and size of synthesized NPs were investigated by transmission electron microscopy (TEM). Samples for TEM (Jeol JEM 1220) imaging were prepared on a carbon grid and the images were taken on high-resolution mode. Crystalinity of NPs were analyzed with X-ray diffraction (XRD, Panalytical EMPYREAN). Fourier transform infrared (FTIR) spectral measurements of NPs as potassium bromide (KBr) pellet were performed using a Perkin Elmer Spectrum Two in the band from 400 to 4000 cm^{-1}.

Plant applications

For surface sterilization, sunflower seeds were treated with %70 EtOH for 3 min and 20% commercial bleaching solution and 2–3 drops of Tween 20 for 20 min and washed several times with distilled water (Dagustu 2018). The seeds were dried and transferred between two filter papers moistened with Hoagland medium (Hoagland and Arnon 1950) in a glass petri dish under sterile and dark conditions for germination at 27 ± 2ºC. When seedlings were visible after 2–3 days, petri plates were kept in 16 h light / 8 h dark cycle at 27 ± 2ºC for 7 days.

When germination was completed, seedlings with equivalent numbers (n = 15) were homogenously distributed in terms of root-shoot length and than transferred to the vessels so as their roots to be soaked into Hoagland medium in the vessels and their leaves to be exposed to light. The media in vessels were aerated with a pump. After the seedlings were left 3 days in vessels including only Hoagland medium (Hoagland and Arnon 1950) for adaptation, NP including media with predetermined concentrations (Table 1) were replenished two times in a week. For the minimum dose

Table 1 Experimental groups for NPs application to sunflower in hydroponic system

Trial no	Experimental groups				
	1(Control 1)	2(Control 2)	3	4	5
1	Hoagland	Hoagland + Bay leaf ext.	Hoagland + 1.5 ppm Fe_2O_3 NP	Hoagland + 5 ppm Fe_2O_3 NP	Hoagland + 20 ppm Fe_2O_3 NP
2	Hoagland	Hoagland + Bay leaf ekx.	Hoagland + 0.5 ppm ZnO NP	Hoagland + 5 ppm ZnO NP	Hoagland + 20 ppm ZnO NP
3	Hoagland	Hoagland + Bay leaf ekx.	Hoagland + 1 ppm TiO_2 NP	Hoagland + 5 ppm TiO_2 NP	Hoagland + 20 ppm TiO_2 NP

determination of Fe_2O_3 and ZnO NPs, elemental content in Hoagland solution, which is a well studied and commonly used medium for several plants, were considered. Since Ti is not an essential element for plants and Hoagland solution does not contain any Ti, reasonable application doses were determined considering the studies given in the literature (Dağhan et al. 2020). NP suspension and medium mixtures were sonicated 1 h at 50 °C before replenishement. Total NP exposure time in vessels was 2 weeks. All experimental groups were allocated for each NP trial as it is shown in Table 1. First control group includes only Hoagland solution containing bulk forms of Fe and Zn as Fe-EDTA and $ZnCl_2$. To ensure the impact of NPs, Fe-EDTA and $ZnCl_2$ content of Hoagland medium was excluded from the ingredients during Fe_2O_3 NP and ZnO NP applications, respectively. Since NPs keep their stability better in the presence of bay leaf extract (ext.), NP synthesis mixtures were directly applied to sunflower. Thus, in order to see the effects that might be arising from bay leaf extract, the second control group includes both Hoagland solution and bay leaf extract considering the minimum amount of it applied to sunflowers with each NP.

Morphological and microscopic (TEM) analysis for investigation of NP uptake by plants

Morhological analyses

After NP treatment, plants were collected and their roots were washed with distilled water. In order to see the effects of NPs on plant growth, leaf and root pictures of the plants were taken and morphological parameters such as root length, shoot length, fresh weight, number of leaves and leaf surface area were measured.

TEM analyses

To detect NP uptake in plant tissues, one of good looking sunflower plants from each Fe_2O_3, ZnO and TiO_2 NP application group with 5 ppm concentration was chosen after 15 days of treatment. Ultra thin sections of plant leaves and roots were prepared and TEM (JEOL JEM 1220) analyses were conducted at Eskişehir Osmangazi University Research Laboratory Application and Research Center (ARUM).

Statistical analysis

Each treatment had 15 biological replicates, as 15 plant/tank. To eliminate the environmental effects such as light and aeration, the pots were shifted twice a week. Data presented under the title of morphological analyses are means ± standard errors of 10 biological replica (n = 10) after 5 outliers were eliminated for each treatment. Statistical analysis was carried out by One-way ANOVA using IBM SPSS Statistics software version 26. After test of homogeneity was applied for the data obtained, significance of results was examined using Tukey's test with 0.05 threshold ($p < 0.05$).

Results

Characterization of synthesized nanoparticles

UV–visible spectroscopic analysis

To measure the absorbance of light beams at different wavelengths with the aid of UV–visible spectroscopy, a spectrum between 190 and 800 nm wavelength was selected. Since analyses were performed with NP suspension in the reaction mixture including bay leaf extract, a control with only bay leaf extract was used. As a result of the analysis it was shown that synthesized Fe_2O_3 NPs produced highest absorbance peaks at 235 nm and 280 nm. The broad absorbance shift in the visible region around 275–295 nm depicts the presence of Fe_2O_3 NPs (Fig. 1a) When the UV–visible spectrum of ZnO NPs synthesized from bay leaf is analyzed, highest absorbance peak was obtained at 335 nm wavelength (Fig. 1b). Considering highest absorption of bulk ZnO observed around 385 nm (Senthilkumar and Sivakumar 2014), a blue shift occured which indicates a decrease in particle size (Fakhari et al. 2019). TiO_2 NPs showed two highest absorbance peaks at 210 nm and 275 nm (Fig. 1c).

Energy bands of the nanoparticles can be estimated using the following equation where k is a constant, α is the absorption coefficient.

$$\alpha = \frac{k(hv - Eg)n/2}{hv}$$

The intercept of the tangent on the Tauc plot obtained from $(\alpha hv)^2$ vs photon energy (hv) gives a direct band gap for n = 1 (Nabi et al. 2020). While similar band gap energy values for Fe_2O_3 and TiO_2 NPs were obtained as 3.47 eV (Fig. 1d) and 3.52 eV (Fig. 1f), repectively, ZnO NPs showed lower band gap energy of 2.92 eV (Fig. 1e).

Dynamic light scattering (DLS)

Hydrodynamic size and size distribution of NP samples were determined by Malvern ZX Zetasizer via DLS. In this method, hydrodynamic diameter of a particle can be determined in relation with Brownian motion (Fahmy 2020). Table 2 compares mean hydrodynamic size and polydispersity index (PDI) values obtained from triplicated DLS analyses against mean geometric diameter size calculated from TEM images. When the geometric and hydrodynamic diameter sizes of NPs compared, hydrodynamic size of both

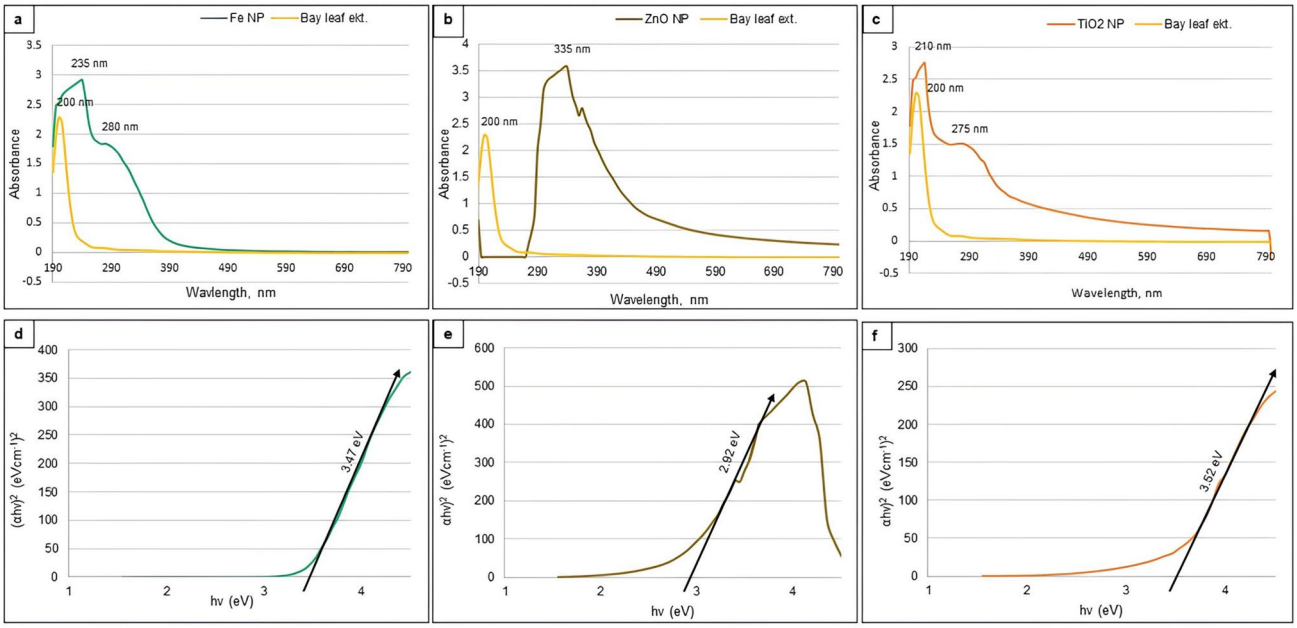

Fig. 1 UV–visible spectra **a**, **b**, **c** and Tauc plot **d**, **e**, **f** of synthesized Fe_2O_3, ZnO and TiO_2 NPs, respectively

Table 2 Geometric and hydrodynamic diameter sizes of NPs

NP	Geometric diameter (nm)	Hydrodynamic diameter (nm)	PDI
Fe_2O_3	14.1 ± 13.0	51 ± 19	0.701 ± 0.10
ZnO	59.8 ± 16.5	144 ± 21	0.665 ± 0.15
TiO_2	86.5 ± 13.1	29 ± 4	0.222 ± 0.03

Fe_2O_3 and ZnO NPs are larger than their geometric size as it is expected due to the hydration shell around NPs in aqueous phase. Interestingly, it was totally opposite for TiO_2 NPs that its hydrodynamic size has approximately been three times less than mean geometric diameter value obtained from the measurements of particle size in TEM image.

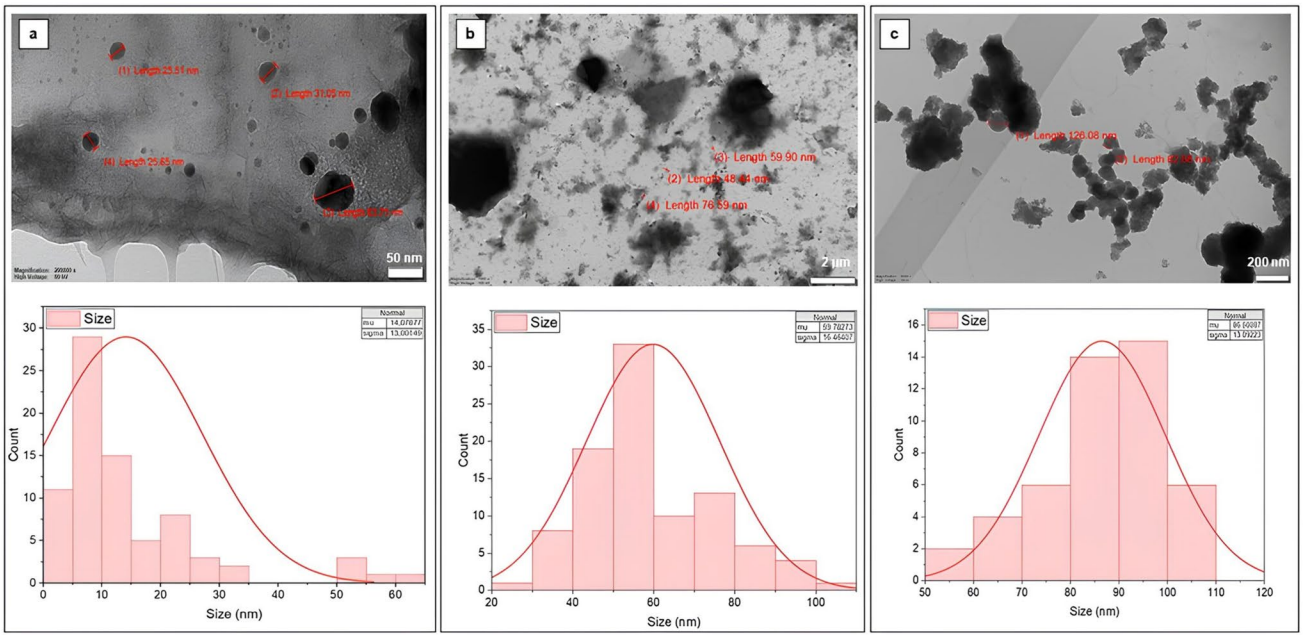

Fig. 2 TEM images and size distribution diagrams of green synthesized **a** Fe_2O_3 NPs, **b** ZnO NPs, **c** TiO_2 NPs

Transmission *electron* microscopy (TEM)

TEM imaging was performed in order to further investigate the morphological characteristics of synthesized NPs. As it can be seen from the Fig. 2a, spherical shaped Fe_2O_3 NPs with a wide range of diameter size distribution from 3 to 61 nm were succesfuly obtained via bay leaf mediated green synthesis. This wide range size distribution verified the high PDI value obtained from DLS analysis. However, most of the Fe_2O_3 NPs have diameter size between 5 and 15 nm. On the other hand, ZnO particles can be seen from Fig. 2b in nano scale varying mostly between 40 and 100 nm and they do not have a uniform morphology. In Fig. 2c, the morphology of TiO_2 NPs are in accordance with the TEM image showing the TiO_2 NPs obtained from *Trachyspermum ammi* in the study of Sunny et al. (2022). Although PDI value seen in DLS analysis were quite low, the diameter of the nanoparticles is changing from 57 to 104 nm, which is higher than the size obtained from DLS analysis. This could be related to the stability of the nanoparticles, since DLS were immediately carried out after the synthesis, the samples were sent to another city for TEM imaging and it took a few days. Considering that TiO_2 has high surface energy and it was not soluble in water, its stability could change and aggregation could occur over some time (Wang et al. 2011).

Fourier transform ınfrared (FTIR) analysis

Figure 3 represents the signals gatherd from KBr pellets of NPs via FTIR spectorcopy. Significant signals around 500–400 cm^{-1} in Fig. 3a–c corresponds to stretching between oxygen and metal elements Fe, Zn and Ti (Vijayakumar et al. 2016). The signals at 3383 cm^{-1}, 3392 cm^{-1} and 3349 cm^{-1} in the FTIR spectrum of Fe_2O_3, ZnO and TiO_2 NPs respectively, indicates O–H stretching vibrations due to the presence of functional groups coming from alcohols, flavonoids, and polyphenols in plant extract. 1615 cm^{-1} in Fig. 3a, 1619 cm^{-1} in Fig. 3b and 1625 cm^{-1} in Fig. 3c indicate the presence of C = C stretching and another common peak around 1046–1099 cm^{-1} resulted from C–C stretching vibrations due to the presence of aromatic groups.

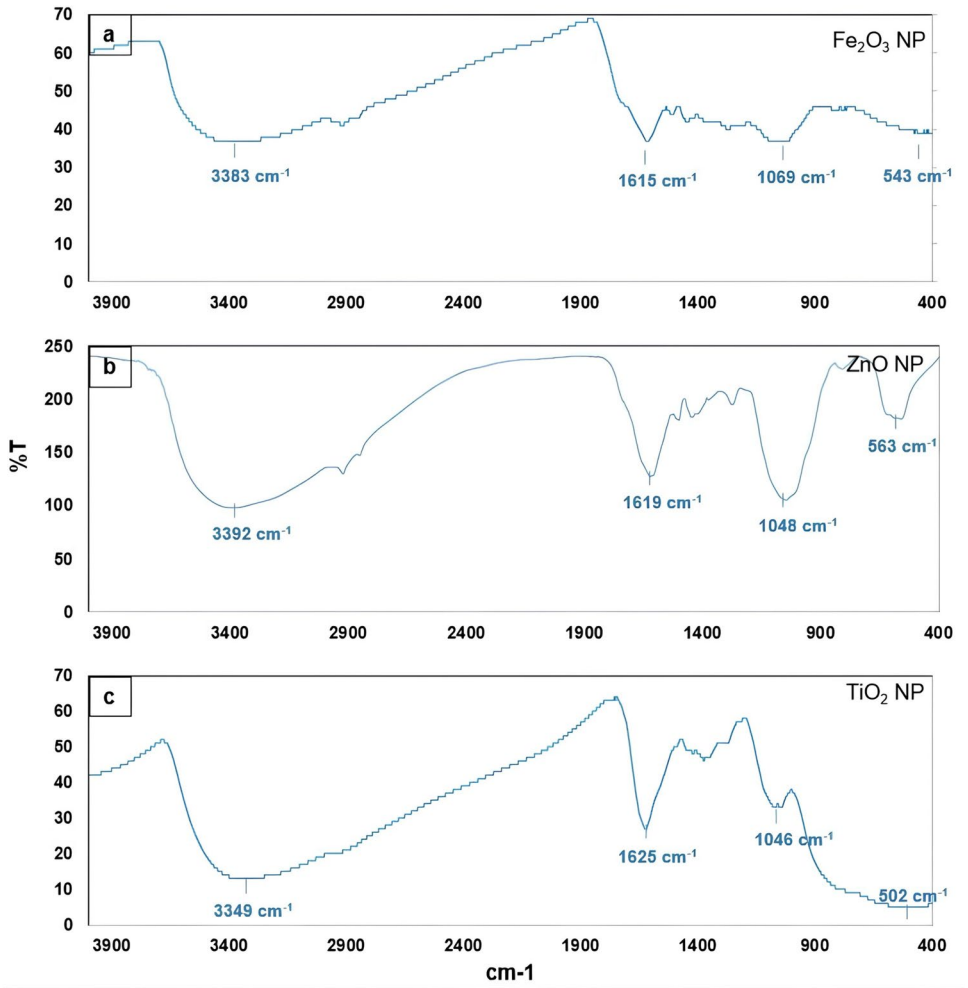

Fig. 3 FTIR spectrums of **a** Fe_2O_3, **b** ZnO, **c** TiO_2NPs

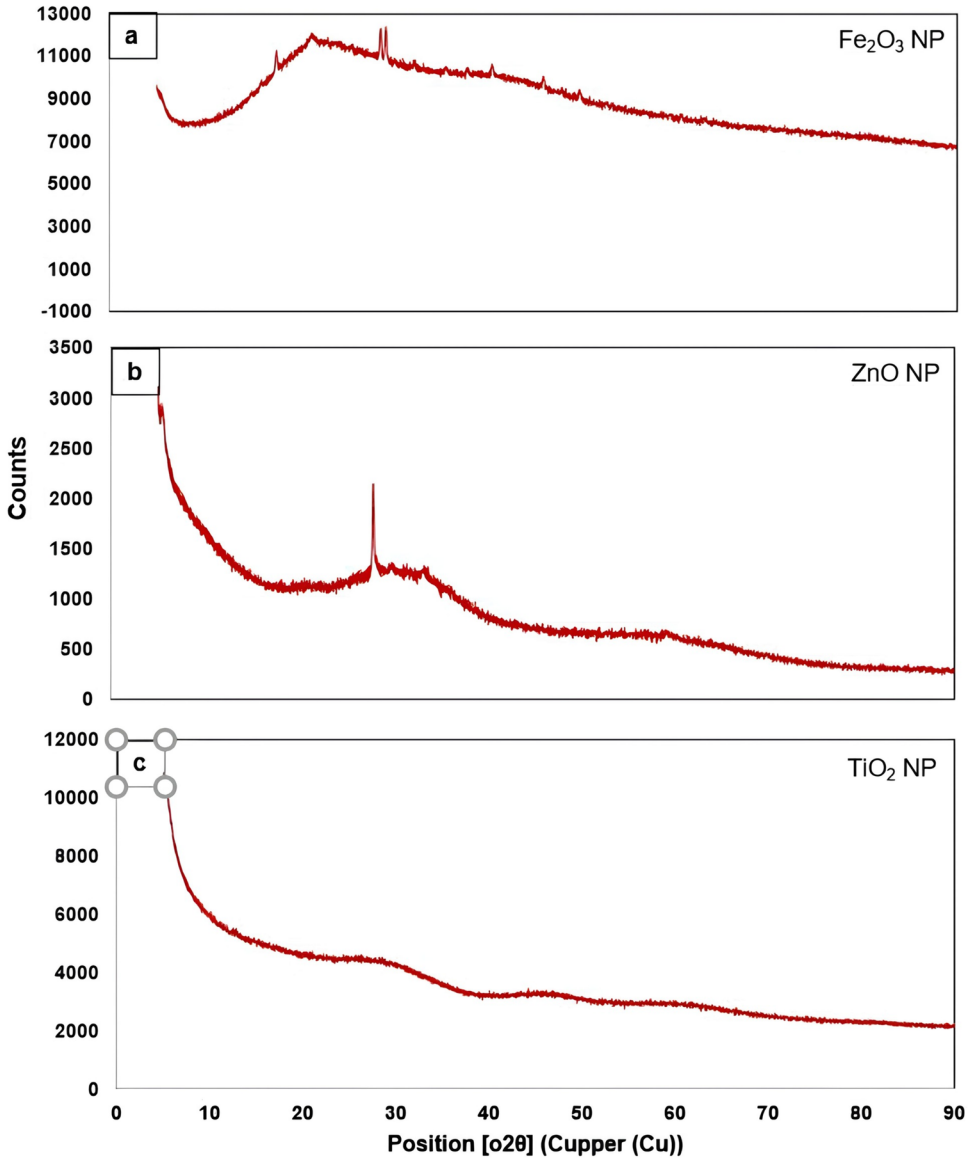

Fig. 4 XRD patterns of **a** Fe_2O_3, **b** ZnO, **c** TiO_2 NPs

X-Ray diffraction (XRD) analysis

XRD patterns for synthesizd NPs have been given in Fig. 4a–c. A peak at 2θ = 35.73° depicted in Fig. 4a most likely corresponds to the presence of iron NPs in the form of maghemite (γ-Fe_2O_3) (Huang et al. 2014). When the whole XRD pattern is compared with XRD patterns of several iron oxide materials reported by Cao et al. (1997) characteristic peaks (2θ = 17.73°, 29.31°, 32.36°, 35.73°, 46.05°, 49.85°, 63.25°) are similar with crystalline Fe_2O_3 rather than its amoprphous form. Figure 4b shows that only one sharp peak at 27.95° and softener peaks around 29.98, 33.30 were obtained, which indicated that ZnO NPs do not have a uniform crystal structure. Similarly, the absence of sharp peaks on XRD pattern (Fig. 4c) corresponds to the amorphous structure of TiO_2 NPs.

Morphological and microscopic (TEM) analysis for investigation of NP uptake by plants

Morphological analysis

After the characterization studies of synthesized Fe_2O_3, ZnO and TiO_2 NPs were completed, sunflower plants were exposed to these NPs with predetermined doses in hydroponic culture. NP + bay leaf extract mixture was directly added into containers including plant groups after 3 days cultivation with only Hoagland medium. And the media were replenished twice a week. At the end of the treatment, pictures of the plant leaves and shoots were taken (Fig. 5,Fig. 6 Fig. 7,Fig. 8, Fig. 9) and several morphological parameters were measured (Fig. 6, Fig. 8, Fig. 10) to discuss the effects of several NP treatments on sunflower.

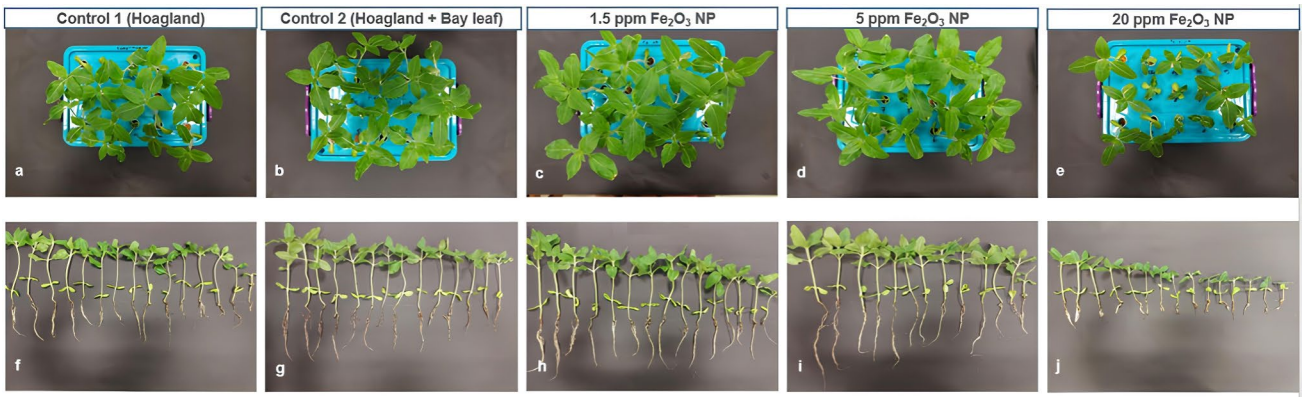

Fig. 5 Results of morphological analysis on sunflower after Fe_2O_3 NP treatment: **a–e** Top view of sunflower plants cultivated in hydroponic system with **a** only Hoagland as Control 1, **b** Hoagland + bay leaf extract as Control 2, **c** 1.5 ppm, **d** 5 ppm, **e** 20 ppm Fe_2O_3 NP application. **f–j** Whole sunflower plants cultivated with **f** only Hoagland as Control 1, **g** Hoagland + bay leaf extract as Control 2, **h** 1.5 ppm, **i** 5 ppm, **j** 20 ppm Fe_2O_3 NP application

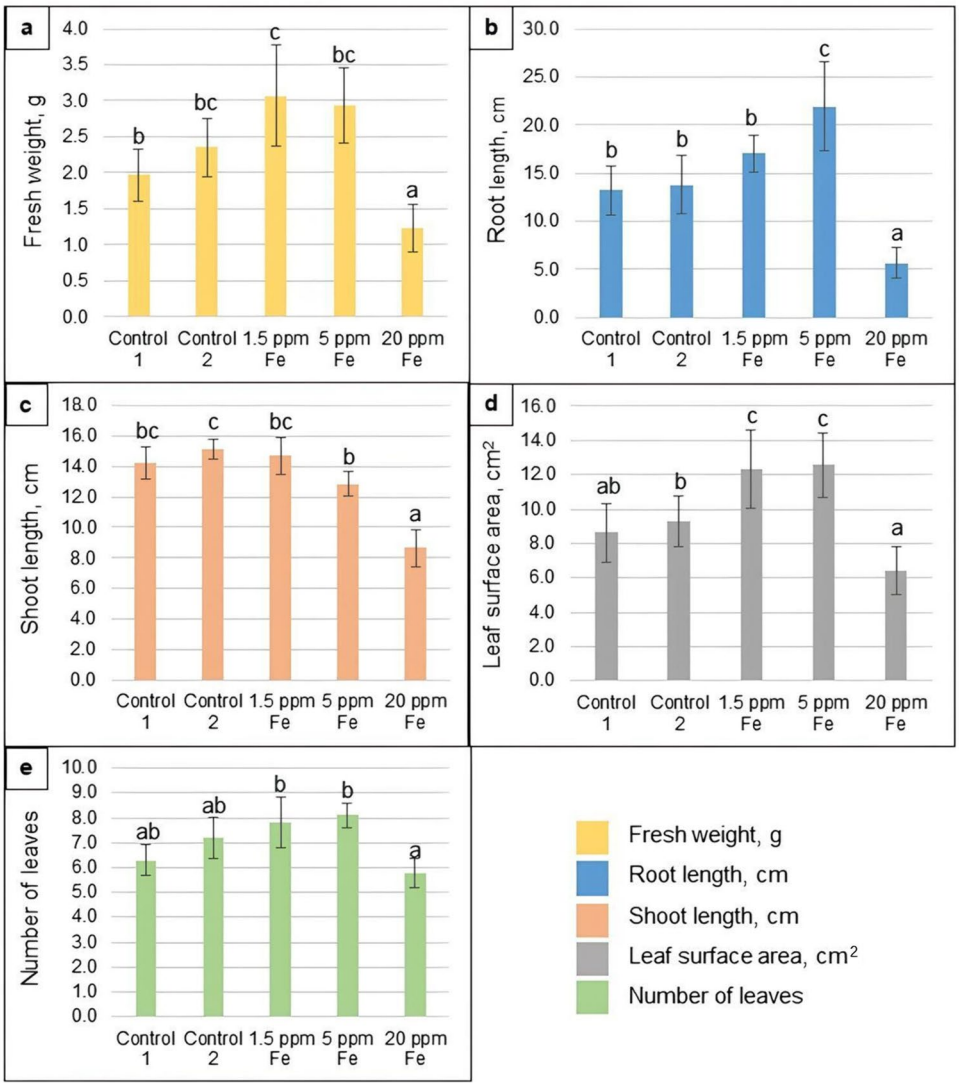

Fig. 6 Graphical illustration of the effects of Fe_2O_3 NP application on sunflower plants in terms of mean **a** fresh weight, **b** root length, **c** shoot length, **d** leaf surface area, **e** number of leaves ($p < 0.05$)

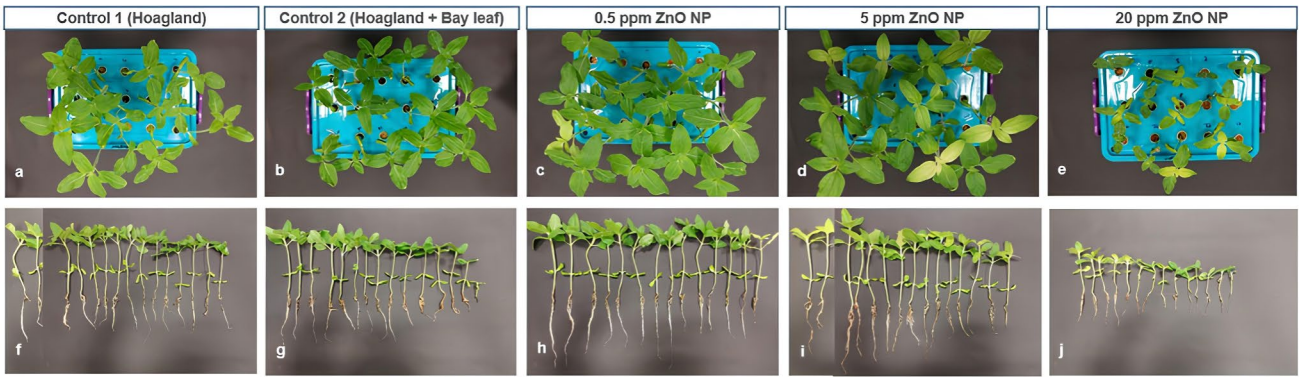

Fig. 7 Results of morphological analysis on sunflower after ZnO NP treatment: **a–e** Top view of sunflower plants cultivated in hydroponic system with **a** only Hoagland as Control 1, **b** Hoagland + bay leaf extract as Control 2, **c** 0.5 ppm, **d** 5 ppm, **e** 20 ppm ZnO NP application. **f–j** Whole sunflower plants cultivated with **f** only Hoagland as Control 1, **g** Hoagland + bay leaf extract as Control 2, **h** 0.5 ppm, **i** 5 ppm, **j** 20 ppm ZnO NP application

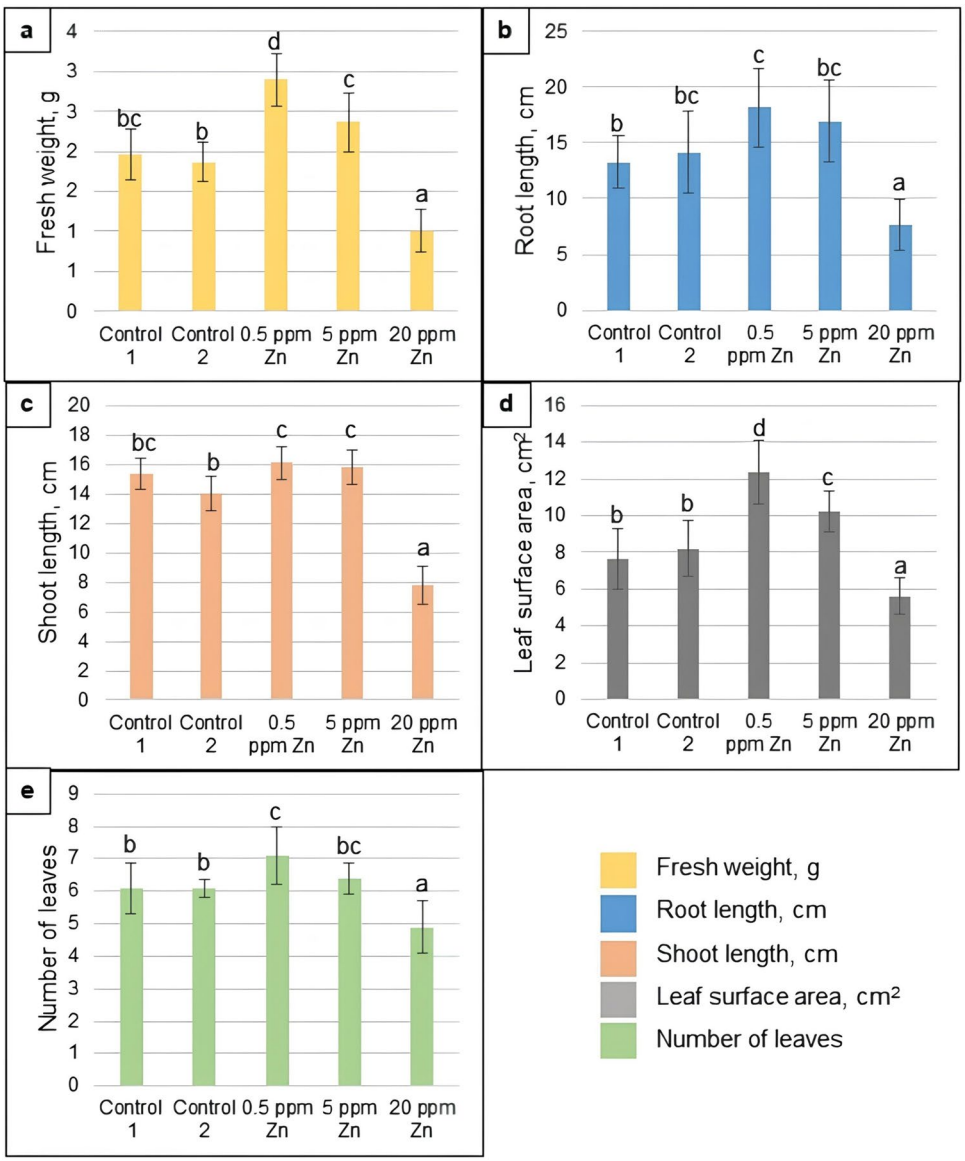

Fig. 8 Graphical illustration of the effects of ZnO NP application on sunflower plants in terms of mean **a** fresh weight, **b** root length, **c** shoot length, **d** leaf surface area, **e** number of leaves ($p < 0.5$)

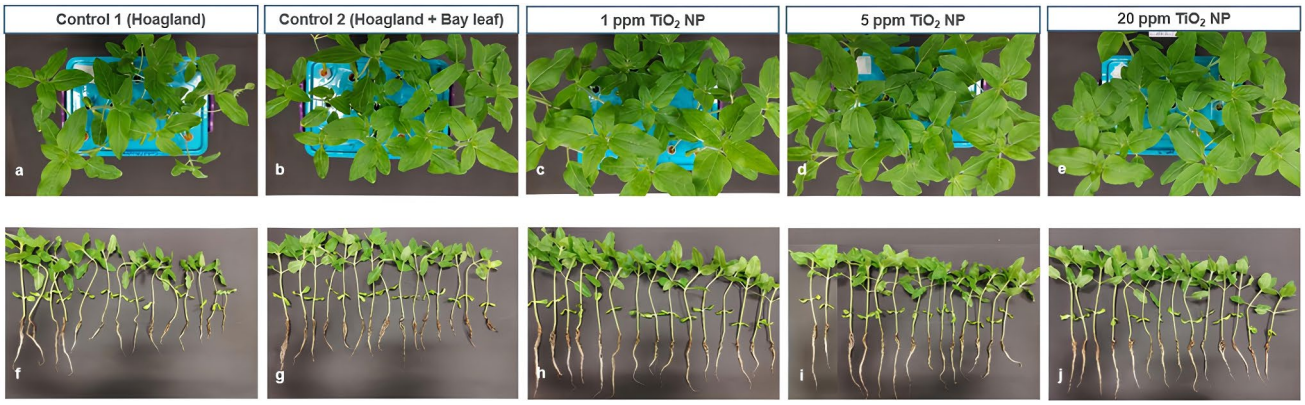

Fig. 9 Results of morphological analysis on sunflower after TiO_2 NP treatment: **a–e** Top view of sunflower plants cultivated in hydroponic system with **a** only Hoagland as Control 1, **b** Hoagland + bay leaf extract as Control 2, **c** 1 ppm, **d** 5 ppm, **e** 20 ppm TiO_2 NP application. **f–j** Whole sunflower plants cultivated with **f** only Hoagland as Control 1, **g** Hoagland + bay leaf extract as Control 2, **h** 1 ppm, **i** 5 ppm, **j** 20 ppm TiO_2 NP application

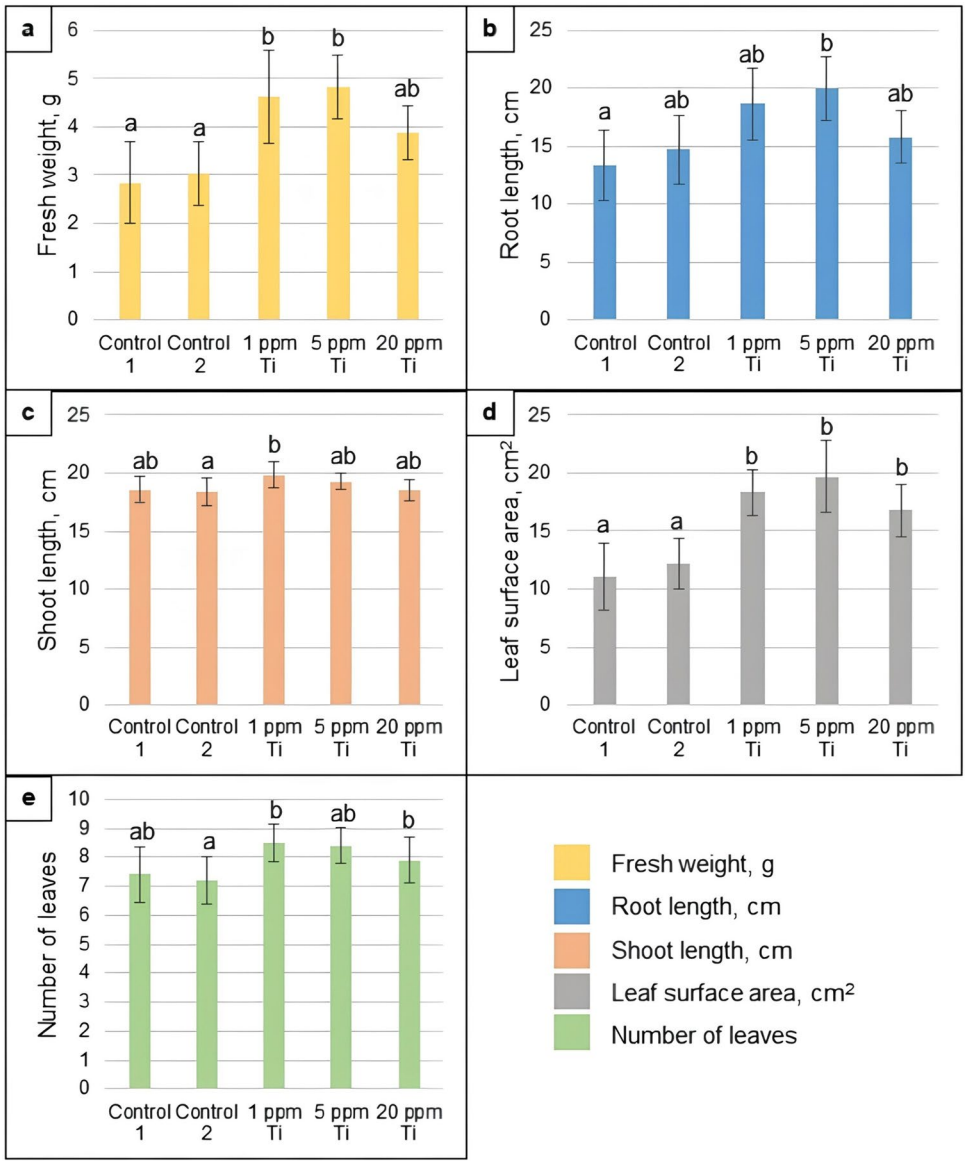

Fig. 10 Graphical illustration of the effects of TiO_2 NP application on sunflower plants in terms of mean **a** fresh weight, **b** root length, **c** shoot length, **d** leaf surface area, **e** number of leaves ($p < 0.5$)

When the measurements were evaluated, it can be generally seen from the Fig. 6a–e that, 1.5—5 ppm Fe_2O_3 NP applications compared to control groups have significant positive effects on several morphological parameters of sunflower cultivated in hydroponic culture and increasing the Fe_2O_3 NP dose to 20 ppm negatively affects most of the parameters. In detail, there has been no statistically meaningful difference between Control 1 and Control 2, indicating that bay leaf extract in related dose has no effect on the plants and results obtained from the groups with NP treatment mostly arise from NP content. However, plant groups treated with 1.5 ppm Fe_2O_3 NP application showed significant improvements in terms of fresh weight (Fig. 6a) and leaf surface area (Fig. 6d). Furthermore, 1.5 ppm was not enough to positively affect the root length (Fig. 6b) compared to control groups, while a significant increase with 5 ppm application was revealed and leaf surface area improvement is as good as 1.5 ppm (Fig. 6d). All these results can be also visually verified from Fig. 5a–e. Leaf surface area of plant groups in 1.5 ppm (Fig. 5c) and 5 ppm (Fig. 5d) treatment seem higher than others and the group treated with 20 ppm Fe_2O_3 NP seems not healthy in terms of both leaf (Fig. 5e) and root (Fig. 5j) morphology.

In sunflower plant groups treated with ZnO NP, it was observed that 0.5 ppm NP application resulted in a highest increment in terms of fresh weight (Fig. 8a), root length (Fig. 8b), leaf surface area (Fig. 8d) and number of leaves (Fig. 8e) relative to other experimental groups. When the concentration is increased to 5 ppm, average leaf surface area of treated sunflower plants was still higher compared to control groups although it was not as high as 0.5 ppm application (Fig. 8d). Further increase of ZnO NP dose to 20 ppm in Hoagland medium caused phytotoxic effects similar to 20 ppm Fe_2O_3 NP application and it is possible to clearly see these results from Fig. 7. In addition, morphological parameters are better in 0.5 and 5 ppm ZnO NP applications, a yellowish color with increasing intensity was seen on some sunflower leaves as parallel to dose increment of applied NPs (Fig. 7d, Fig. 7e).

In TiO_2 NP application groups, 1 ppm and 5 ppm TiO_2 NP treatment obviously increased average fresh weight (Fig. 10a) and leaf surface area (Fig. 10a) compared to the control groups. Figure 9 also showed that the leaves of TiO_2 NP applied groups have a larger surface area. In addition, there is no significant difference of measured parameters between 20 ppm TiO_2 NP treatment and other doses (Fig. 10). Thus, TiO_2 NPs up to 20 ppm in Hoagland solution have no toxic effect in terms of morphological parameters unlike 20 ppm Fe_2O_3 and 20 ppm ZnO NP applications.

Microscopic (TEM) analysis

For the investigation of NP uptake by sunflower, samples taken from roots and leaves of NP treated plants were imaged with TEM. The roots of experimental groups can be compared from Fig. 11. Black dots depicted with red arrows supposed to be NPs since control group representing no NP application (Fig. 11a, Fig. 11b) via lack of these dots. From this point of view, it was obvious that there is no accumulation in the root of control group. Hovewer, there is a clear accumulation of Fe_2O_3 NPs by root cell wall and cellular structures still keep their healty morphology and structural integrity (Fig. 11c, d) Spherical shape of uptaken NPs by plant roots correlate with morphology of synthesized Fe_2O_3 NPs presented in previous TEM image (Fig. 2). Similar situation can be seen for TiO_2 NP application. Figures 11g, h showed that TiO_2 NPs were localized inner cell wall and cytoplasm and structural integrity seem to be protected. In ZnO NP application, on the other side, cell wall of the cells

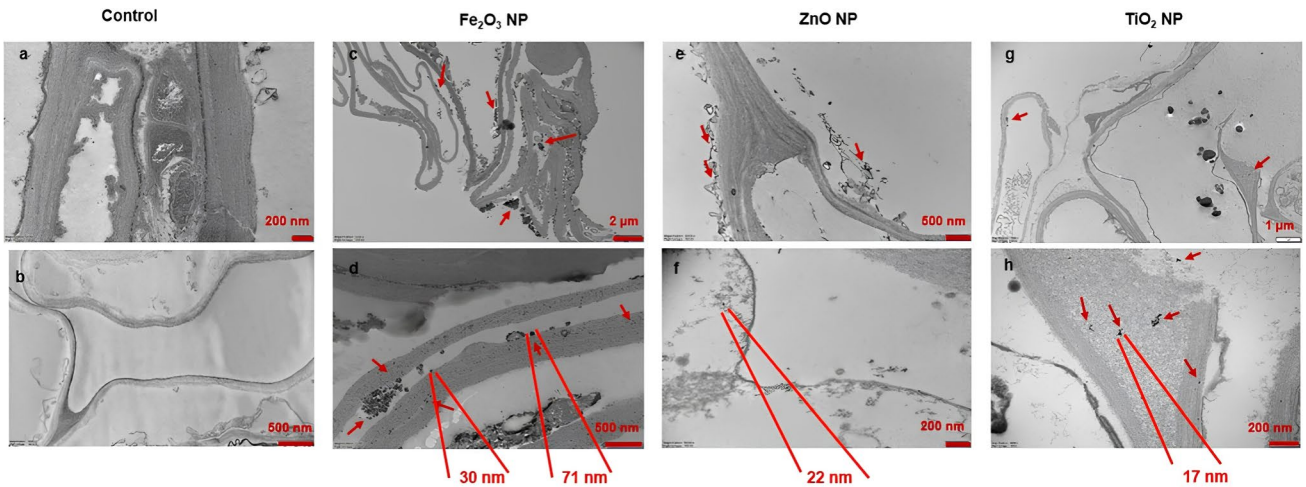

Fig. 11 TEM images taken from root sections of sunflower plants treated with **a-b** no NP, **c-d** Fe_2O_3 NP, **e–f** ZnO NP, **g-h** TiO_2 NP

seems to lose their integrity with the accumulation of ZnO NPs (Fig. 11e, f).

The particle size of Fe_2O_3, ZnO and TiO_2 NPs localized in the root sections were measured by Image J program around 30—71 nm, 22 nm and 17 nm, respectively (Fig. 11). It is obvious that particle sizes for Fe_2O_3 and TiO_2 NPs here corraleted with their hydrodynamic diameter size obtained from DLS analysis, rather than their geometric sizes estimated from TEM images of purified NP samples (Table 2.) Knowing that NPs are applied to the plants in aqueous form and a hydration shell surrounds NPs, it makes sense that the size of uptaken particles seem larger here. Furthermore, NPs with various sizes were encountered in the root section treated with Fe_2O_3 NPs (Fig. 11d). This result correlates with high PDI value of synthesized Fe_2O_3 NPs obtained from DLS analysis and confirms the uniform distribution of NP size (Table 2).

When the images taken from leaf samples were evaluated, similar effects can be seen in roots. There is no NP accumulation in the control group showing good cell wall integrity (Fig. 12). In Fe_2O_3 (Fig. 12c, d) and TiO_2 (Fig. 12g, h) NP applications, even though it is very rare relative to root samples, there is NP localization in the cytoplasm and cellular morphologies were still regular. Also in the leaves of sunflower plants treated with ZnO NP (Fig. 12e, f), contrary to root images (Fig. 11e, f) cellular organelles seem healthy. Accordingly, all NP types seem to be uptaken and translocated through the leaves by sunflower plants.

Discussion

Synthesis of metallic Fe_2O_3, ZnO and TiO_2 NPs from bay leaf (*Laurus nobilis*) extract as an environment friendly reducing agent was performed and their effects on the physiological growth parameters of sunflower under hydroponic system were investigated in this study. Protection of the NP stability during applications is a common challenge due to their high surface energy and tendency to aggregate (Shrestha et al. 2020). Knowing that plant extracts not only reduce the NPs but also help maintain their stability (Dikshit et al. 2021), of the reaction mixture including both NPs and bay leaf extract, and was directly applied sunflower, unlike in other studies.

When the characterization analyses after NP synthesis evaluated, UV visible spectrum of sythesized NPs showed highest absorbance peaks at characteristic wavelength numbers. Highest peak at 280 nm in Fig. 1a indicates the presence of Fe NP. Data from literature confirms our results. In the study of Sathishkumar et al. (2018) magnetic Fe_3O_4 NPs synthesized from *C. guianensis* extract produces a strong absorbance in visible region around 250–350 nm. Jamzad and Kamari Bidkorpeh. (2020) also reported that absorption at 285 nm was obtained for α-Fe_2O_3 synthesized from *Laurus nobilis* leaf extract. In another study, iron oxide nanoparticles synthesized from *Avicennia marina* flower extract similarly gave peak at 298–301 nm (Karpagavinayagam and Vedhi 2019). For ZnO NPs, highest absorbance at 335 nm was obtained (Fig. 1b). In accordance with this result, Fakhari et al. (2019) also revealed that a blue shift occured in the absorption spectra of green synthesized ZnO NPs from *Laurus nobilis* (Fakhari et al. 2019). In another study carried out by Azizi et al. (2014), a sharp absortion

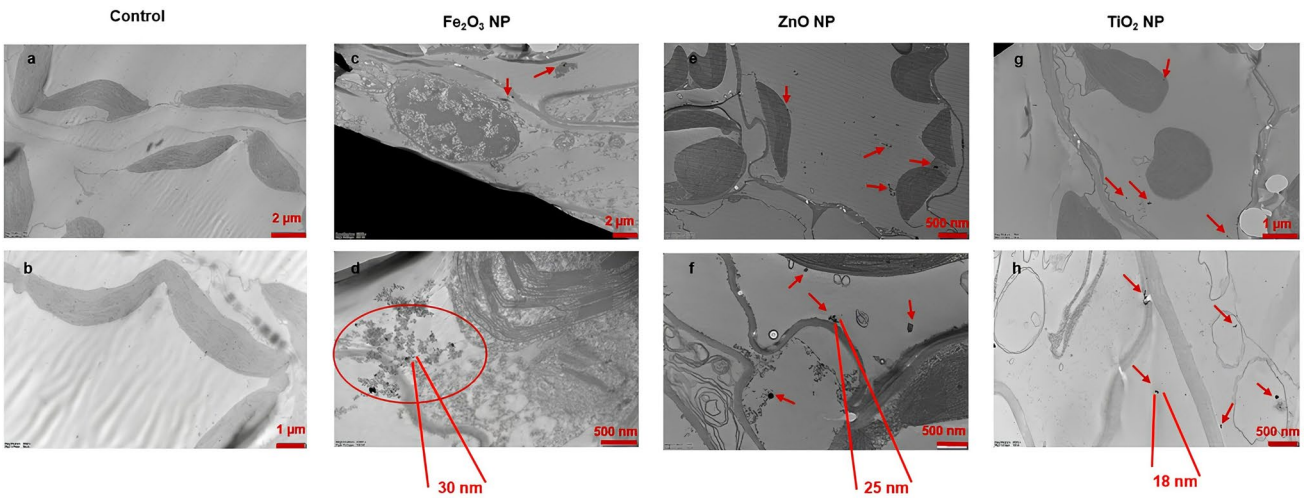

Fig. 12 TEM images taken from leaf sections of sunflower plants treated with **a-b** no NP, **c-d** Fe_2O_3 NP, **e–f** ZnO NP, **g-h** TiO_2 NP

in the wavelength of 334 nm was obtained for ZnO NPs synthesized using brown marine macroalga *Sargassum muticum* aqueous extract. In absorption spectroscopy, there is an opposite relation between band gap and particle size. While it is known that absorption for the bulk form of ZnO is usually around 385 nm (Senthilkumar and Sivakumar 2014), decrease in wavelength of absorption showed that ZnO NPs with smaller particle size are present (Fakhari et al. 2019). TiO_2 NPs, on the other hand, showed two highest absorbance peaks at 210 nm and 275 nm (Fig. 1c). Similarly, Hassan et al. (2020) reported highest absorbance at 270 nm and 290 nm for TiO_2 NPs relative to two different plant leaf extracts (*Strychnos spinosa* and *Blighia sapida*). In addition, following a similar synthesis methodology (Dobrucka 2017), TiO_2 NPs exhibited elevated absorbance at 280 nm with increased pH of the plant extract solution. The peak at 235 nm in the spectrum of Fe_2O_3 NP and the peak at 210 nm in the spectrum of TiO_2 NP might arise from the strong coordination between the hydroxyl group containing plant biomaterials and transition metals (Sathishkumar et al. 2018).

The band gap energy can give clues about size and photocatalitic activity of particles. There is an inverse proportion between the band gap energy and size of nanoparticles (Fakhari et al. 2019). The band gap increases with decreasing particle size while the absorption edge is shifted to a higher energy and the smaller particle size could enhance the photocatalitic activity (Pavithra et al. 2023). In accordance with the blue shifts from 400 nm to 270–280 nm in UV-spectra of Fe_2O_3 and TiO_2 NPs they have similar band gap as 3.47 eV and 3.52 eV, respectively (Fig. 1d, f). Gautam et al. (2018) reported that iron nanoparticles synthesized from the extract of waste tea showed a lower band gap energy as 2.99 eV. Nabi et al. (2020) represented a similar band gap energy for TiO_2 NPs synthesized from cinnamon powder. ZnO NPs on the other hand showed a lower band gap energy of 2.92 eV as parallel to the highest absorbance pek at around 335 nm (Fig. 1e). This indicates ZnO NPs have larger particle size compared to Fe_2O_3 and TiO_2. In another study by Alamdari et al. (2020) ZnO NPs with 3.3 eV band gap energy was synthesized using leaf extract of *Sumbucus ebulus*. Although highest absorbance was observed at a higher wavelength (around 376 nm), band gap energy is higher compare to the value obtained in this study. This could cause from an earlier shift around 500 nm in the UV spectrum of bay leaf extract mediated green synthesized ZnO NPs, even if the highest absorbance peak observed at 335 nm (Fig. 1b).DLS analyses (Table 2) revealed the mean hydrodynamic size of all synthesized NPs are less than 150 nm. However, PDI values, which represents the relative distribution of particle size should be also considered. PDI represents the homogenity and uniformity of the particle size distribution and it is expected to be less than 0.5 if a narrow and homogenous distribution of size is desired. Data obtained from DLS analysis shows that size distribution of TiO_2 NPs are quite homogenous while Fe_2O_3 and ZnO NPs are a bit far from the homogenity with a wider size distribution. However, hydrodynamic conditions and agglomeration of particles can affect the DLS measurements. Therfore, data obtained from DLS should be interpreted together with TEM images (Fahmy 2020). High PDI in DLS analysis is a common case for NPs synthesized via plant extracts since their size and shape are highly variable (Ying et al. 2022). Gao et al. (2016) reported that the particle sizes of nano zero valent iron nanoparticles synthesized via grape seeds vary from 63 to 381 nm. The maximum size distribution of ZnO NPs after *Pongamia pinnata* extract mediated synthesis was found to be around 90 nm with a range starting from 10 to 120 nm (Sundrarajan et al. 2015). In another study carried out by Rajeswari et al. (2021), the hydrodynamic size of TiO_2 NPs synthesized from *Laurus nobilis* was reported as 441 nm according to the measurements by DLS, while the primary size found to be around 100 nm. Compared to this result, TiO_2 NPs synthesized in our study showed a pretty much lower size distribution around 29 ± 4 nm with a very low polydispersity (0.022 ± 0.03).

Morphology and size of synthesized NPs were verified with TEM imaging. Figure 2a showed that Fe_2O_3 NPs with spherical shape and 14.1 nm mean diameter size were successfully synthesized. Particles showed a similar size distribution with the bay leaf mediated Fe_2O_3 NPs synthesized by Jamzad and Kamari Bidkorpeh (2020), however, a more uniform spherical shape characteristic were obtained while they have both spherical like and hexagonal shaped particles. Near particle size was also reported for the green synthesis with Carob pod as 7 nm (Demirezen et al. 2019). Furthermore, cubic Fe NPs with higher particle size (45.09 nm) synthesized in another study in which *Avicennia marina* flower extract was used as reducing agent (Karpagavinayagam and Vedhi 2019). The morphology of TiO_2 NPs shown in Fig. 2c are in accordance with the TEM image showing TiO_2 NPs obtained from *Trachyspermum ammi* in the study of Sunny et al. (2022). Although PDI value seen in DLS analysis were quite low, the geometric diameter of the nanoparticles is changing from 58 to 110 nm, which is higher than the size obtained from DLS analysis (Table 2). This could be related to the stability of the nanoparticles, since DLS were immediately carried out after the synthesis, the samples were sent to another city for TEM imaging and it took a few days. Considering that TiO_2 has high surface energy and it is not soluble in water, its stability could change and aggregation can occur over some time during purification procedure before the analyses (Wang et al. 2011).

FTIR analysis (Fig. 3) also revealed supportive results corresponding to the presence of interactions between compounds coming from plant extract and NP precursors.

Characteristic absorption peaks identified in the literature correlate with our results. Jamzad and Kamari Bidkorpeh (2020) similarly reported that peaks at 600 and 450 cm^{-1} in the FTIR spectrum of Fe_2O_3 NPs synthesized from *Laurus nobilis* indicate Fe–O stretching vibrations in the hematite phase. Vijayakumar et al. (2016) synthesized ZnO NPs via plant leaf extract, and the absorption peak at 413 cm^{-1} was identified as a standard peak due to Zn–O stretching vibrations. In another study conducted for the synthesis of TiO_2 NPs, a band at around 638 cm^{-1} was shown to be indicative of O–Ti–O skeletal frequency (Sharfudeen et al. 2017).

When XRD patterns of synthesized NPs evaluated (Fig. 4), Fe_2O_3 NPs showed more crystalline like structure while ZnO and TiO_2 NPs are more likely amorphous, since any characteristic sharp peaks did not found out for them. According to Jamzad and Kamari Bidkorpeh (2020), heat treatment after *L. nobilis* mediated synthesis of Fe_2O_3 NPs and heat treatment at 250 °C for 12 h showed sharp characteristics corresponding crystalline nature. On the contrary, an extra heat treatment was not applied to Fe NPs in this study and softer peaks were obtained (Fig. 4a). However, characteristic peaks are still similar with crystalline Fe_2O_3 rather than its amoprphous form according to the data given by Cao et al. (1997).

The absence of specific sharp peaks in XRD pattern of ZnO and TiO_2 NPs (Fig. 4b, c) means that they have amorphous structure rather than crystalline. Most of the plant mediated NPs are purified and heat application is performed for the crystallization to obtain stabilized and uniform morphology of the particles. However, amorphous NPs have larger surface area and higher reactivity compare to crystalline NPs. This property make them useful for several appliacation areas such as medicine and environmental remediation (Yadav et al. 2022). In addition, Larue et al. (2012) announce that crystallinity does not influence the transfer of NPs after they investigated the effect of rutile and anatase form of TiO_2 NPs on wheat in terms of translocation from root to shoot.

After characterization studies of the synthesized Fe_2O_3, ZnO and Ti NPs were completed, sunflower plants were exposed to these NPs with predetermined doses in hydroponic culture. Figure 6 shows that Fe_2O_3 NP application significantly affect the fresh weight, rooth length and leaf surface area in a positive manner while it starts to show toxic effects after 20 ppm. This shows the importance of appropriate dose in fertilizer applications. In accordance with our results, Martínez-Fernández et al. (2016) revealed in their study that 50 mg/L and 100 mg/L application of nanomagemite (Fe_2O_3 NP) in hydroponic culture reduced root hydrolic conductivity, nutrient uptake and chlorophyll content of sunflower plants. In another study of Martínez-Fernández et al. (2015), however, in soil amended with 1% Fe_2O_3 NP promote the growth of *Helianthus annuus* dry weight. According to Rawat et al. (2017), foliar treatment of 4 ppm iron sulfide nanoparticle solution at 30 days after sowing brought maximal enhancement in agronomic attributes of *B. juncea*. In another study (Iannone et al. 2016) citric acid coated Fe_3O_4 NPs were found as not phytotoxic for wheat and it was denoted that they could potentially be beneficial for the design of new agricultural products.

In ZnO NP treated sunflower groups, similarly, all parameters except shoot length were significantly improved and 20 ppm caused decrease in all parameters (Fig. 8). Kolenčík et al. (2020) also revealed similar results in their study with a difference in treatment method. They denoted that foliar application of 2.6 mg/L ZnO-NPs induced generally better physiological responses by sunflower. In another study conducted by Seleiman et al. (2020) it was denoted that foliar application of 60 mg/L Zn NP enhanced growth, physiological, and yield characteristics of sunflowers grown in soil irrigated with polluted wastewater. In addition, Sharma et al. (2022) applied ZnO NPs to *Zea mays* L. via both seed priming and foliar application. They indicated that seed priming with 200 ppm ZnO NP enhanced germination percentage and seed vigor index, while 200 ppm ZnO NP foliar application provide a better physiological status with increased stem diameter and leaf surface area. Furthermore it was proved that transport of Zn element through the plant is faster compared to $ZnSO_4$ as control. Although 200 ppm ZnO NP result improvements in several parameters, 400 ppm concentration was reported as phytotoxic for plant attributes. In this present study, while morphological parameters are better in 0.5 and 5 ppm Zn NP applications, a yellowish color with a rising intensity were seen on some sunflower leaves as parallel to dose increment of applied NPs (Fig. 7d, e). This indicates Zn toxicity as it is reported by Blamey et al. (1997) that high Zn uptake can cause yellow chlorosis on upper leaves of sunflower.

TiO_2 NPs, on the other hand, have gained attention as new generation nanofertilisers in agriculture. Altough there are doubts about their potential toxicity. Several studies have revealed beneficial results with TiO_2 NP application on plants (Kolenčík et al. 2020). In accordance with these studies, our results indicates that 1 ppm and 5 ppm Ti NP treatment obviously increased average fresh weight (Fig. 10a) and leaf surface area (Fig. 10d). Furthermore, TiO_2 NPs up to 20 ppm in Hoagland solution have no toxic effect in terms of morphological parameters unlike 20 ppm Fe_2O_3 and 20 ppm ZnO NP applications. Results of the experiments conducted by Kolenčík et al. (2020) supports our results. They reported that foliar application of 2.6 mg/L Ti NPs to sunflower plants under field conditions had no negative effect on number of plants and seed heads and improvement in the common physiological parameters at stem elongation and flower-bud formation stage were seen two weeks after the first foliar TiO_2 NP

application. In another study conducted by Janmohammadi et al. (2017), the highest number of achenes per head, greatest kernel weight in sunflower plants after spraying with TiO_2 NPs were reported. Enhancing effects of TiO_2 NPs on growth characteristics of other plant species have also been revealed. Shenavaie et. al, (2022) reported that 150 mg/L TiO_2 NP application significantly improved parameters such as shoot length, shoot weight, relative water content, chlorphyll content and menthol content in peppermint (*Mentha piperita* L). It is thought that TiO_2 NPs probably enhances the water flow from the root to the shoot and supports the uptake of minerals and nitrogen metabolism.

Morphological changes in NP treated plant groups show that NPs were uptaken by plants. In order to verify this, TEM images of plant tissues were obtained and NPs were detected in both roots and leaves of treated plants. Cell integrity of 5 ppm Fe_2O_3 (Fig. 11c, Fig. 12c), and TiO_2 (Fig. 11g, Fig. 12g) NP treated plants look normal from TEM images of plant tissues. Similar results were obtained in the study of Tombuloglu et al. (2019) reporting the translocation of magnetite (Fe_3O_4) nanoparticles from root to shoot in barley (*Hordeum vulgare* L.). Although cellular penetration in leaves was not observed, positive effects in plant growth and phenological parameters such as chlorophyll, total soluble protein, number of chloroplasts, dry weight were obtained. Miyoko Kubo-Irie et al. (2016) also reports that TiO_2 NPs were observed in root vascular tissue of *Aristolochia debilis* and thus with diameters smaller than 100 nm may cross the cellulose layer. ZnO NP treated plants, on the other hand, seem to lose their cell integrity due to the toxic effect of 5 ppm dose (Fig. 11e, Fig. 12e). The particle diameter size for uptaken NPs from roots are estimated as 30 and 71 nm for Fe_2O_3 (Fig. 11d), 22 nm for ZnO (Fig. 11f) and 17 nm for TiO_2 (Fig. 11h) NPs, which are consistent with hydrodynamic diameter sizes of nanoparticles determined by DLS analysis (Table 2). However, particle size for ZnO NPs detected in root tissue sections (Fig. 11f) are quite smaller than both mean geometric size and hydrodynamic diameter size. In addition, particle sizes of ZnO and TiO_2 NPs uptaken by roots and translocated through the leaves are in consistence with each other. In the leaves of Fe_3O_4 NP treated plants, only NPs with smaller size seem to be translocated (Fig. 12d) while NPs with various size from 30 to 71 nm were encountered in root sections (Fig. 11d). In accordance with these results, Larue et al. (2012) reported that NP diameter size influences the transfer plant tissues. Their study, in which wheat was exposed to TiO_2 NPs with diameters ranging from 14 to 655 nm, revealed that diameter size up to 140 nm can accumulate in roots but 36 nm was threshold for translocation through the shoot.

Conclusion

To the best of our knowledge, this is the first study to investigate the effects of bay leaf -mediated green synthesized Fe_2O_3, ZnO and Ti NPs on sunflower.

Characterization studies showed that NPs were successfully synthesized using an environment friendly method by utilizing bay leaf extract as a reducing agent instead of harmful chemical reagents. UV spectrum and FTIR analysis exhibited characteristic peaks indicating the presence of the desired NPs, while DLS analysis and TEM images confirmed successful synthesis. After completing the characterization studies, green-synthesized nanoparticles were applied to sunflower plants under hydroponic conditions, and their uptake and effects on morphological parameters were assessed. Unlike other studies, NPs, without any purification step, were directly added to the hydroponic system to improve the stability of NPs in the presence of bay leaf extract as a capping agent. This approach not only provided significant cost and effort savings but also ensured stability during application. TEM images of the samples obtained from the plants confirmed the uptake and translocation of NPs from root to leaf. Furthermore, improvements in morphological parameters of sunflower plants were observed after NP treatment with appropriate concentrations. Fe_2O_3, ZnO, and Ti NP applications on sunflower up to 5 ppm generally improved root length, fresh weight, and leaf surface area compared to control groups, including bulk forms of Fe and Zn, while 20 ppm caused a significant decrease in morphological parameters.

Our findings demonstrate the potential of the bay leaf mediated green synthesized Fe_2O_3, ZnO and TiO_2 NPs as new constituents for biofertilizers, offering alternatives to their conventional forms. Poor soil fertility (lack of essential minerals), disease attacks and pesticide infestations are some of the major constrains that affect sunflower production yield. From this perspective, these preliminary results can lead to novel studies for further evaluation of the synthesized Fe_2O_3, ZnO and TiO_2 NPs regarding their effects on sunflower oil seed production yield and their response to various biotic and abiotic stress factors.

Acknowledgements This study was supported by Marmara University, Scientific Research Projects Commission with the FDK-2023-10885 project number.

Author contributions GU, YA, and AAU designed the study, TOC performed the experiments and data analysis. All authors wrote, read and approved the final manuscript.

Data availability All data are available in the article.

Declarations

Conflict of interest The author declares no conflict of interest, financial or otherwise.

Ethical approval This article does not contain any studies with human participants or animals performed by the author.

Consent to participant Not applicable.

Consent to publish Not applicable.

References

Abobatta WF (2018) Nanotechnology application in agriculture. Acta Sci Agric 2(6):99–102

Adeleke BS, Babalola OO (2020) Oilseed crop sunflower (*Helianthus annuus*) as a source of food: nutritional and health benefits. Food Sci Nutr 8(9):4666–4684. https://doi.org/10.1002/fsn3.1783

Alamdari S, Sasani Ghamsari M, Lee C, Han W, Park HH, Tafreshi MJ, Aferideh H, Ara MHM (2020) Preparation and characterization of zinc oxide nanoparticles using leaf extract of *Sambucus ebulus*. Appl Sci 10(10):3620. https://doi.org/10.3390/app10103620

Alamdari S, Mirzaee O, Jahroodi FN, Tafreshi MJ, Ghamsari MS, Shik SS, Ara MHM, Lee KY, Park HH (2022) Green synthesis of multifunctional ZnO/chitosan nanocomposite film using wild *Mentha pulegium* extract for packaging applications. Surf Interfaces 34:102349. https://doi.org/10.1016/j.surfin.2022.102349

Alidoust D, Isoda A (2013) Effect of γFe_2O_3 nanoparticles on photosynthetic characteristic of soybean (*Glycine max* (L.) Merr): foliar spray versus soil amendment. Acta Physiol Plant 35(12):3365–3375. https://doi.org/10.1007/s11738-013-1369-8

Ashraf SA, Siddiqui AJ, Abd Elmoneim OE, Khan MI, Patel M, Alreshidi M, Moin A, Singh R, Snoussi M, Adnan M (2021) Innovations in nanoscience for the sustainable development of food and agriculture with implications on health and environment. Sci Total Environ 768:144990. https://doi.org/10.1016/j.scitotenv.2021.144990

Azizi S, Ahmad MB, Namvar F, Mohamad R (2014) Green biosynthesis and characterization of zinc oxide nanoparticles using brown marine macroalga *Sargassum muticum* aqueous extract. Mater Lett 116:275–277. https://doi.org/10.1016/j.matlet.2013.11.038

Badouin H, Gouzy J, Grassa CJ, Murat F, Staton SE, Cottret L, Legrand L (2017) The sunflower genome provides insights into oil metabolism, flowering and Asterid evolution. Nature 546(7656):148–152. https://doi.org/10.1038/nature22380

Beheshtkhoo N, Kouhbanani MAJ, Savardashtaki A, Amani AM, Taghizadeh S (2018) Green synthesis of iron oxide nanoparticles by aqueous leaf extract of *Daphne mezereum* as a novel dye removing material. Appl Phys A 124(5):363–369. https://doi.org/10.1007/s00339-018-1782-3

Blamey FPC, Zollinger RK, Schneiter AA (1997) Sunflower production and culture. Sunflower Technol Prod 35:595–670. https://doi.org/10.2134/agronmonogr35.c12

Cao X, Prozorov R, Koltypin Y, Kataby G, Felner I, Gedanken A (1997) Synthesis of pure amorphous Fe_2O_3. J Mater Res 12:402–406. https://doi.org/10.1557/JMR.1997.0058

Chemingui H, Missaoui T, Chékir Mzali J, Yildiz T, Konyar M, Smiri M, Saidi N, Hafiane A, Yatmaz HC (2019) Facile green synthesis of zinc oxide nanoparticles (ZnO NPs): Antibacterial and photocatalytic activities. Mater Res Exp 6(10):1050b4. https://doi.org/10.1088/2053-1591/ab3cd6

Dağhan H, Gülmezoğlu N, Köleli N, Karakaya B (2020) Impact of titanium dioxide nanoparticles (TiO_2-NPs) on growth and mineral nutrient uptake of wheat (*Triticum vulgare* L.). Biotech Stud 29(2):69–76. https://doi.org/10.38042/biost.2020.29.02.03

Dagustu N (2018) In vitro tissue culture studies in sunflower (*Helianthus* spp.). Ekin J Crop Breed Genetic 4(1):13–21

Demirezen DA, Yıldız YŞ, Yılmaz DD (2019) Amoxicillin degradation using green synthesized iron oxide nanoparticles: kinetics and mechanism analysis. Environ Nanotechnol Monit Manag 11:100219. https://doi.org/10.1016/j.enmm.2019.100219

Dikshit PK, Kumar J, Das AK, Sadhu S, Sharma S, Singh S, Gupta PK, Kim BS (2021) Green synthesis of metallic nanoparticles: applications and limitations. Catalysts 11(8):902. https://doi.org/10.3390/catal11080902

Dimitrijevic A, Horn R (2018) Sunflower hybrid breeding: from markers to genomic selection. Front Plant Sci 8:2238. https://doi.org/10.3389/fpls.2017.02238

Dobrucka R (2017) Synthesis of titanium dioxide nanoparticles using *Echinacea purpurea* herba. Iran J Pharm Res 16(2):753–759

Fahmy HM (2020) Oxidative impact of carob leaf extract–synthesized iron oxide magnetic nanoparticles on the kidney, liver, testis, and spleen of wistar rats. BioNanoSci 10(1):54–61. https://doi.org/10.1007/s12668-019-00704-1

Fakhari S, Jamzad M, Kabiri Fard H (2019) Green synthesis of zinc oxide nanoparticles: a comparison. Green Chem Lett Rev 12(1):19–24. https://doi.org/10.1080/17518253.2018.1547925

Gangwar J, Kadanthottu Sebastian J, Puthukulangara Jaison J, Kurian JT (2023) Nano-technological interventions in crop production—A review. Physiol Mol Biol Plants 29(1):93–107. https://doi.org/10.1007/s12298-022-01274-5

Gao JF, Li HY, Pan KL, Si CY (2016) Green synthesis of nanoscale zero-valent iron using a grape seed extract as a stabilizing agent and the application for quick decolorization of azo and anthraquinone dyes. RSC Adv 6(27):22526–22537. https://doi.org/10.1039/C5RA26668H

Gulya T, Harveson R, Mathew F, Block C, Thompson S, Kandel H, Markell S (2019) Comprehensive disease survey of US sunflower: disease trends, research priorities and unanticipated impacts. Plant Dis 103(4):601–618. https://doi.org/10.1094/PDIS-06-18-0980-FE

Gutiérrez-Ramírez JA, Betancourt-Galindo R, Aguirre-Uribe LA, Cerna-Chávez E, Sandoval-Rangel A, Ángel ECD, Chacón-Hernández JC, Chacón-Hernández JI, Hernández-Juárez A (2021) Insecticidal effect of zinc oxide and titanium dioxide nanoparticles against Bactericera cockerelli sulc.(*hemiptera*: *Triozidae*) on tomato Solanum lycopersicum. Agronomy 11(8):1460. https://doi.org/10.3390/agronomy11081460

Hassan H, Omoniyi KI, Okibe FG, Nuhu AA, Echioba EG (2020) Assessment of wound healing activity of green synthesized titanium oxide nanoparticles using *Strychnos Spinosa* and *Blighia sapida*. J Appl Sci Environ Manage 24(2):197–206. https://doi.org/10.4314/jasem.v24i2.2

Hoagland DR, Arnon DI (1950) The water-culture method for growing plants without soil. Calif Agric Exp Stn Circ 347(2):32. https://doi.org/10.5555/19500302257

Huang L, Weng X, Chen Z, Megharaj M, Naidu R (2014) Synthesis of iron-based nanoparticles using oolong tea extract for the degradation of malachite green. Spectrochim Acta A Mol Biomol Spectrosc 117:801–804. https://doi.org/10.1016/j.saa.2013.09.054

Hussain M, Farooq S, Hasan W, Ul-Allah S, Tanveer M, Farooq M, Nawaz A (2018) Drought stress in sunflower: physiological effects and its management through breeding and agronomic alternatives. Agric Water Manag 201:152–166. https://doi.org/10.1016/j.agwat.2018.01.028

Hussain A, Oves M, Alajmi MF, Hussain I, Amir S, Ahmed J, Rehman T, El-Seedi HR, Ali I (2019) Biogenesis of ZnO nanoparticles

using *Pandanus odorifer* leaf extract: anticancer and antimicrobial activities. RSC Adv 9(27):15357–15369. https://doi.org/10.1039/c9ra01659g

Iannone MF, Groppa MD, de Sousa ME, van Raap MBF, Benavides MP (2016) Impact of magnetite iron oxide nanoparticles on wheat (*Triticum aestivum* L.) development: evaluation of oxidative damage. Environ Exp Bot 131:77–88. https://doi.org/10.1016/j.envexpbot.2016.07.004

Ishak NM, Kamarudin SK, Timmiati SN (2019) Green synthesis of metal and metal oxide nanoparticles via plant extracts: an overview. Mater Res Express 6(11):112004. https://doi.org/10.1088/2053-1591/ab4458

Jamzad M, Kamari Bidkorpeh M (2020) Green synthesis of iron oxide nanoparticles by the aqueous extract of *Laurus nobilis* L. leaves and evaluation of the antimicrobial activity. J Nanostruct Chem 10(3):193–201. https://doi.org/10.1007/s40097-020-00341-1

Janmohammadi M, Yousefzadeh S, Dashti S, Sabaghnia N (2017) Effects of exogenous application of nano particles and compatible organic solutes on sunflower (*Helianthus annuus* L.). Botanica Serbica 41(1):37–46. https://doi.org/10.5281/zenodo.453554

Kabir AH, Tahura S, Elseehy MM, El-Shehawi AM (2021) Molecular characterization of Fe-acquisition genes causing decreased Fe uptake and photosynthetic inefficiency in Fe-deficient sunflower. Sci Rep 11(1):1–13. https://doi.org/10.1038/s41598-021-85147-z

Karpagavinayagam P, Vedhi C (2019) Green synthesis of iron oxide nanoparticles using *Avicennia marina* flower extract. Vacuum 160:286–292. https://doi.org/10.1016/j.vacuum.2018.11.043

Kaya Y, Jocic S, Miladinovic D (2012) Sunflower. In: Gupta SK (ed) Technological innovations in major world oil crops, Volume 1: breeding. Springer New York, New York, NY, pp 85–129. https://doi.org/10.1007/978-1-4614-0356-2_4

Kolenčík M, Ernst D, Urík M, Ďurišová Ľ, Bujdoš M, Šebesta M, Kratošová G (2020) Foliar application of low concentrations of titanium dioxide and zinc oxide nanoparticles to the common sunflower under field conditions. Nanomater 10(8):1619. https://doi.org/10.3390/nano10081619

Kubo-Irie M, Yokoyama M, Shinkai Y, Niki R, Takeda K, Irie M (2016) The transfer of titanium dioxide nanoparticles from the host plant to butterfly larvae through a food chain. Sci Rep 6:23819. https://doi.org/10.1038/srep23819

Lahuf AA, Alfarttoosi HA, Al-Sweedi TM, Middlefell-Williams JE (2019) Evaluation of an integration between the nanosized zinc oxide and two cultivars for the control of damping-off disease in sunflower crop. Res Crops 20(1):174–179. https://doi.org/10.31830/2348-7542.2019.024

Larue C, Laurette J, Herlin-Boime N, Khodja H, Fayard B, Flank AM, Carriere M (2012) Accumulation, translocation and impact of TiO_2 nanoparticles in wheat (*Triticum aestivum* spp.): influence of diameter and crystal phase. Sci Total Environ 431:197–208. https://doi.org/10.1016/j.scitotenv.2012.04.073

Li J, Hu J, Ma C, Wang Y, Wu C, Huang J, Xing B (2016) Uptake, translocation and physiological effects of magnetic iron oxide (γ-Fe_2O_3) nanoparticles in corn (*Zea mays* L.). Chemosphere 159:326–334. https://doi.org/10.1016/j.chemosphere.2016.05.083

Louarn J, Boniface MC, Pouilly N, Velasco L, Pérez-Vich B, Vincourt P, Muños S (2016) Sunflower resistance to broomrape (*Orobanche cumana*) is controlled by specific QTLs for different parasitism stages. Front Plant Sci 7:590. https://doi.org/10.3389/fpls.2016.00590

Martínez-Fernández D, Vítková M, Bernal MP, Komárek M (2015) Effects of nano-maghemite on trace element accumulation and drought response of *Helianthus annuus* L. in a contaminated mine soil. Water Air Soil Pollut 226(4):1–9. https://doi.org/10.1007/s11270-015-2365-y

Martínez-Fernández D, Barroso D, Komárek M (2016) Root water transport of *Helianthus annuus* L. under iron oxide nanoparticle exposure. Environ Sci Pollut Res 23(2):1732–1741. https://doi.org/10.1007/s11356-015-5423-5

Moosa AA, Jaafar JN (2017) Green reduction of graphene oxide using tea leaves extract with applications to lead ions removal from water. Nanosci Nanotechnol 7(2):38–47. https://doi.org/10.5923/j.nn.20170702.03

Mystrioti C, Xanthopoulou TD, Tsakiridis P, Papassiopi N, Xenidis A (2016) Comparative evaluation of five plant extracts and juices for nanoiron synthesis and application for hexavalent chromium reduction. Sci Total Environ 539:105–113. https://doi.org/10.1016/j.scitotenv.2015.08.091

Nabi G, Raza W, Tahir MB (2020) Green synthesis of TiO_2 nanoparticle using cinnamon powder extract and the study of optical properties. J Inorg Organomet Polym 30:1425–1429. https://doi.org/10.1007/s10904-019-01248-3

Pavithra S, Bessy TC, Bindhu MR, Venkatesan R, Parimaladevi R, Alam MM, Mayandi J, Umadevi M (2023) Photocatalytic and photovoltaic applications of green synthesized titanium oxide (TiO_2) nanoparticles by *Calotropis gigantea* extract. J Alloys Compd 960:170638. https://doi.org/10.1016/j.jallcom.2023.170638

Pérez-Vich B, Akhtouch B, Knapp SJ, Leon AJ, Velasco L, Fernández-Martínez JM, Berry ST (2004) Quantitative trait loci for broomrape (*Orobanche cumana* Wallr.) resistance in sunflower. Theor Appl Genet 109(1):92–102. https://doi.org/10.1007/s00122-004-1599-7

Pilorgé E (2020) Sunflower in the global vegetable oil system: situation, specificities and perspectives. OCL 27:34. https://doi.org/10.1051/ocl/2020028

Rajiv P, Rajeshwari S, Venckatesh R (2013) Bio-Fabrication of zinc oxide nanoparticles using leaf extract of *Parthenium hysterophorus* L. and its size-dependent antifungal activity against plant fungal pathogens. Spectrochim Acta A Mol Biomol Spectrosc 112:384–387. https://doi.org/10.1016/j.saa.2013.04.072

Rawat M, Nayan R, Negi B, Zaidi MGH, Arora S (2017) Physio-biochemical basis of iron-sulfide nanoparticle induced growth and seed yield enhancement in *B. juncea*. Plant Physiol Biochem 118:274–284. https://doi.org/10.1016/j.plaphy.2017.06.021

Sabaghnia N, Javanmard A, Janmohammadi M, Nouraein M (2018) The influence of nano-TiO_2 and nano-silica particles effects on yield and morphological traits of sunflower. Helia 41(69):213–225. https://doi.org/10.1515/helia-2018-0010

Said MT, Mohamed Noaman H (2021) Effect of foliar spraying time by different micronutrients nanoparticles on sunflower yield and its attributes. Assiut J Agric Sci 52(3):22–35. https://doi.org/10.21608/ajas.2021.95041.1044

Sathishkumar G, Logeshwaran V, Sarathbabu S, Jha PK, Jeyaraj M, Rajkuberan C, Senthilkumar N, Sivaramakrishnan S (2018) Green synthesis of magnetic Fe_3O_4 nanoparticles using *Couroupita guianensis* Aubl. fruit extract for their antibacterial and cytotoxicity activities. Artif Cell Nanomed 46(3):589–598. https://doi.org/10.1080/21691401.2017.1332635

Seleiman MF, Alotaibi MA, Alhammad BA, Alharbi BM, Refay Y, Badawy SA (2020) Effects of ZnO nanoparticles and biochar of rice straw and cow manure on characteristics of contaminated soil and sunflower productivity, oil quality, and heavy metals uptake. Agronomy 10(6):790. https://doi.org/10.3390/agronomy10060790

Senthilkumar SR, Sivakumar T (2014) Green tea (*Camellia sinensis*) mediated synthesis of zinc oxide (ZNO) nanoparticles and studies on their antimicrobial activities. Int J Pharm Pharm Sci 6(6):461–465

Sethy NK, Arif Z, Mishra PK, Kumar P (2020) Green synthesis of TiO_2 nanoparticles from *Syzygium cumini* extract for photocatalytic removal of lead (Pb) in explosive industrial wastewater. Green Process Synth 9(1):171–181. https://doi.org/10.1515/gps-2020-0018

Sharma P, Urfan M, Anand R, Sangral M, Hakla HR, Sharma S, Bhagat M (2022) Green synthesis of zinc oxide nanoparticles using Eucalyptus lanceolata leaf litter: characterization, antimicrobial and agricultural efficacy in maize. Physiol Mol Bio Plants 28(2):363–381. https://doi.org/10.1007/s12298-022-01136-0

Shenavaie Zare A, Ganjeali A, Vaezi Kakhki MR, Cheniany M, Mashreghi M (2022) Plant elicitation and TiO_2 nanoparticles application as an effective strategy for improving the growth, biochemical properties, and essential oil of peppermint. Physiol Mol Bio Plants 28(7):1391–1406. https://doi.org/10.1007/s12298-022-01215-2

Shrestha S, Wang B, Dutta P (2020) Nanoparticle processing: Understanding and controlling aggregation. Adv Colloid Interface Sci 279:102162. https://doi.org/10.1016/j.cis.2020.102162

Sundrarajan M, Ambika S, Bharathi K (2015) Plant-extract mediated synthesis of ZnO nanoparticles using Pongamia pinnata and their activity against pathogenic bacteria. Adv Powder Technol 26(5):1294–1299. https://doi.org/10.1016/j.apt.2015.07.001

Sunny NE, Mathew SS, Kumar SV, Saravanan P, Rajeshkannan R, Rajasimman M, Vasseghian Y (2022) Effect of green synthesized nano-titanium synthesized from *Trachyspermum ammi* extract on seed germination of *Vigna radiate*. Chemosphere 300:134600. https://doi.org/10.1016/j.chemosphere.2022.134600

Tassi E, Giorgetti L, Morelli E, Peralta-Videa JR, Gardea-Torresdey JL, Barbafieri M (2017) Physiological and biochemical responses of sunflower (*Helianthus annuus* L.) exposed to nano-CeO_2 and excess boron: modulation of boron phytotoxicity. Plant Physiol Biochem 110:50–58. https://doi.org/10.1016/j.plaphy.2016.09.013

Tauqeer HM, Turan V, Farhad M, Iqbal M (2022) Sustainable agriculture and plant production by virtue of biochar in the era of climate change. In: Mirza H, Jalal AG, Kamrun N (eds) Managing plant production under changing environment. Springer Nature Singapore, Singapore, pp 21–42. https://doi.org/10.1007/978-981-16-5059-8_2

Tombuloglu H, Slimani Y, Tombuloglu G, Almessiere M, Baykal A (2019) Uptake and translocation of magnetite (Fe_3O_4) nanoparticles and its impact on photosynthetic genes in barley (*Hordeum vulgare* L.). Chemosphere 226:110–122. https://doi.org/10.1016/j.chemosphere.2019.03.075

Verma SK, Das AK, Patel MK, Shah A, Kumar V, Gantait S (2018) Engineered nanomaterials for plant growth and development: a perspective analysis. Sci Total Environ 630:1413–1435. https://doi.org/10.1016/j.scitotenv.2018.02.313

Wang C, Mao H, Wang C, Fu S (2011) Dispersibility and hydrophobicity analysis of titanium dioxide nanoparticles grafted with silane coupling agent. Ind Eng Chem Res 50(21):11930–11934. https://doi.org/10.1021/ie200887x

Yadav VK, Gnanamoorthy G, Ali D, Bera SP, Roy A, Kumar G, Basnet A (2022) Cytotoxicity, removal of Congo red dye in aqueous solution using synthesized amorphous iron oxide nanoparticles from incense sticks ash waste. J Nanomater 2022:1–12. https://doi.org/10.1155/2022/5949595

Ying S, Guan Z, Ofoegbu PC, Clubb P, Rico C, He F, Hong J (2022) Green synthesis of nanoparticles: current developments and limitations. Environ Technol Inno 26:102336. https://doi.org/10.1016/j.eti.2022.102336